Eur. J. Wood Prod. (2010) 68: 341–350
DOI 10.1007/s00107-010-0463-5

ORIGINALS ORIGINALARBEITEN

Quantitative determination of bound water diffusion in multilayer boards by means of neutron imaging

Walter Sonderegger · Stefan Hering · David Mannes · Peter Vontobel · Eberhard Lehmann · Peter Niemz

Received: 6 April 2010 / Published online: 10 July 2010

Abstract Diffusion processes into multilayered samples of Norway spruce (*Picea abies* [L.] Karst.) exposed to a differentiating climate (dry side/wet side) were determined and quantified by means of neutron imaging (NI). The experiments were carried out at the neutron imaging facility NEUTRA at the Paul Scherrer Institute (PSI) in Villigen (Switzerland).

With NI the influence of different adhesives (polyvinyl acetate (PVAc), urea formaldehyde resin (UF), epoxy resin (EP), one-component polyurethane (1C PUR)) on the diffusion process could be determined by varying the layer number and the thickness of adhesive joints of the samples. Thereby, neutron transmission images were used to measure time dependent water profiles in the diffusion direction. Using Fick's second law, diffusion coefficients for radial and tangential water transport in spruce wood and in the adhesive joints were calculated depending on moisture content (MC). It was found that the diffusion coefficients of the adhesives (1C PUR, EP at high MC) were up to three orders of magnitude lower than those of spruce wood. PVAc and UF had a smaller barrier effect compared to wood, which in contrast to 1C PUR and EP, clearly depends on the MC.

This article is dedicated to Gerd Wegener on the occasion of his retirement as professor at the Technische Universität München.

W. Sonderegger (✉) · S. Hering · P. Niemz
Department of Civil, Environmental and Geomatic Engineering, Institute for Building Materials, ETH Zurich, 8093 Zurich, Switzerland
e-mail: wsonderegger@ethz.ch

D. Mannes · P. Vontobel · E. Lehmann
Spallation Neutron Source (ASQ), Paul Scherrer Institute (PSI), 5232 Villigen, Switzerland

Quantitative Bestimmung der Diffusion von gebundenem Wasser in mehrlagigen Brettlamellen mittels Neutronenradiographie

Zusammenfassung Es wurden Diffusionsprozesse an mehrlagigen Proben von Fichte (*Picea abies* [L.] Karst.), welche einem Differenzklima (trocken/feucht) ausgesetzt waren, mittels Neutronenradiographie untersucht und quantifiziert. Die Experimente wurden an der Radiographiestrahllinie NEUTRA am Paul Scherrer Institut (PSI) in Villigen (Schweiz) durchgeführt.

Mittels Neutronenradiographie konnte der Einfluss verschiedener Klebstoffe (Polyvinylacetat (PVAc), Harnstoffharz (UF), Epoxidharz (EP) und Einkomponenten-Polyurethan (1K-PUR)) auf den Diffusionsprozess bestimmt werden, indem die Anzahl und die Dicke der Klebfugen variiert wurden. Dabei wurden Neutronen-Transmissionsbilder verwendet, womit zeitabhängige Profile in Diffusionsrichtung gemessen werden konnten. Anhand des zweiten Fick'schen Gesetzes konnten die Diffusionskoeffizienten für die Klebstoffe sowie für Fichte in radialer und tangentialer Richtung in Abhängigkeit der Feuchte berechnet werden. Dabei wiesen die Klebstoffe (1K-PUR, EP bei hohen Feuchten) bis zu drei Zehnerpotenzen niedrigere Diffusionskoeffizienten als Fichtenholz auf. Bei PVAc und UF war die Sperrwirkung gegenüber dem Holz geringer und es zeigte sich im Gegensatz zu 1K-PUR und EP eine deutliche Abhängigkeit von der Holzfeuchte.

1 Introduction

In recent years, glued solid wood materials such as glued laminated timber (glulam) used as girder or multilayered solid wood panels used for walls and ceilings have gained

in importance. In this context, the diffusion of water vapour within wood and the barrier effect of adhesive joints are of high relevance to the field of building physics: this particularly is the case regarding the hygroscopic behaviour and the water transfer in building elements and the humidity exchange with the room. While diffusion processes of wood are subject of many investigations (e.g. Stamm 1959a, 1959b; Kollmann and Côté 1968; Skaar 1988; Siau 1995; Frandsen et al. 2007), the influence of adhesive joints on the diffusion processes has scarcely been studied. One of the few studies done on this topic was carried out by Frühwald (1973). He investigated in detail the influence of bond lines of a phenolic resin between the veneers of beech plywood by varying the number of bond lines and films per line. Recently, Foglia (2006) investigated the influence of bond lines of a one-component polyurethane adhesive between spruce wood lamellas on the water vapour resistance using the cup method according to ISO 12572 (2001). Based on these data (resistance factors of spruce wood without bond lines and with 2, 3 and 5 bond lines), the water vapour resistance factor of the bond lines could be calculated according to the Glaser method (Glaser 1959). This resulted in a mean water vapour resistance factor of 3900 for the wet cup test and 8700 for the dry cup test. This indicates a high dependence of the adhesive's water vapour resistance on the moisture content (MC) of the adjacent wood, as already stated by Frühwald (1973) for a phenolic resin.

The goal of this study was to investigate the phenomenon of the moisture-depending diffusion resistance for different adhesives: polyvinyl acetate (PVAc), urea formaldehyde resin (UF), epoxy resin (EP) and one-component polyurethane (1C PUR). Neutron radiography was used to detect the water content within wood (according to Mannes et al. 2009b). The advantage of this non-destructive method is its high sensitivity to hydrogen allowing visualisation of time-dependent water diffusion processes in wood. In the recent past, several investigations with neutron radiography were carried out in order to analyse the capillary water absorption by partial immersion of wood specimen into water (Lehmann et al. 2001a; Niemz et al. 2002; Mannes et al. 2006). Mannes et al. (2009b) demonstrated that even small amounts of water absorbed from air moisture can be detected and quantified.

2 Material and methods

2.1 Material

20 samples from Norway spruce (*Picea abies* [L.] Karst.) of approximately 120 mm (length) × 15 mm (width) × 30 mm (height) were prepared for testing bound water diffusion. The diffusion process was run from the top to the bottom of the sample. Two of the samples were used for determination of the radial and tangential diffusion. The other 18 samples were added with one to five bond lines at half height or rather regularly distributed over the height in order to determine the influence of bond lines on the diffusion processes. For these samples, the diffusion in the spruce wood occurs in the tangential direction.

The samples were tested in two series. Series 1 included the two samples without adhesives and samples with 1, 3 or 5 bond lines of UF and 1C PUR. The applied adhesives are commonly used for load-bearing timber structures, UF (cold gluing) in dry conditions and 1C PUR even in humid conditions. Series 2 includes samples with bond lines of EP, PVAc, UF and 1C PUR; the thickness of the bond lines was varied (0.1 mm, 0.5 mm, 1.0 mm). EP is a two component adhesive of high strength, PVAc allows many general applications in the wooden industry and 1C PUR—in contrast to that one of series 1—is an elastic adhesive for parquet flooring. The used UF of series 2 is the same as in series 1. All adhesive joints were prepared at 20 °C and 65% relative humidity (RH). Table 1 gives an overview of all tested samples.

2.2 Methods

2.2.1 Experimental setup

The experiments were performed at the neutron radiography facility NEUTRA of the spallation neutron source SINQ at the Paul Scherrer Institute (PSI) in Villigen, Switzerland (Lehmann et al. 2001b). The samples were tested in two series over a period of about ten weeks. The detailed test conditions for the two series are described in Table 2. During this time, the preliminarily oven-dried samples were exposed to a differentiating climate (series 1: 20 °C/85% RH to almost 0% RH; series 2: 20 °C/90% RH to almost 0% RH); the moisture of the samples was measured with neutron radiation after defined time intervals in order to follow the diffusion process into the sample.

Thereby, at the beginning of the tests the samples (dried at 103 °C until weight constancy) are insulated with aluminium tape on the four edges, leaving only the top and the bottom planes (the orthogonal planes of the required diffusion direction) unsealed. Each sample is then fixed on a cup filled with silica gel that is closed with a slotted aluminium plate. The sample sits above the opening of the slot, which has the same length and width as the sample (Fig. 1). The first neutron radiation measurement is still made for the dry sample so as to obtain a reference image.

For the measurement, the cup with the sample is positioned in front of the neutron detector (a combination of a neutron sensitive ^{6}Li doped ZnS scintillator and a CCD-camera) so that the tangential-longitudinal plane (and in one

Table 1 Overview of the tested samples and the applied adhesives at the beginning of the measurements (oven-dry) and the mean moisture content ($MC_{mean.end}$) and water concentration ($C_{mean.end}$), respectively at the end of the measurements after 70 days (series 1) or 74 days (series 2) exposed to a differentiating climate (series 1: 20 °C/85% RH to 0% RH; series 2: 20 °C/90% RH to 0% RH)
Tab. 1 Überblick über die untersuchten Proben und die verwendeten Klebstoffe zu Beginn der Messungen (darrtrocken) sowie deren mittlerer Feuchtegehalt ($MC_{mean.end}$) bzw. Wasserkonzentration ($C_{mean.end}$) am Ende der Messungen, nachdem die Proben 70 Tage (Serie 1) bzw. 74 Tage (Serie 2) einem Differenzklima ausgesetzt worden waren (Serie 1: 20 °C/85 % rLF zu 0 % rLF; Serie 2: 20 °C/90 % rLF zu 0 % rLF)

	Material/adhesive	No.	Direction of diffusion	Bond line No. (–)	Thickness of the bond line (mm)	Oven-dry height (mm)	Oven-dry density (kg/m^3)	$MC_{mean.end}$ (%)	$C_{mean.end}$ (g/m^3)
Series 1	Spruce wood	1	Tangential	–	–	29.1	418	12.8	0.054
		2	Radial	–	–	29.9	402	12.5	0.050
	Urea-1	3	Tangential	1	0.1	29.0	398	12.5	0.050
		4	Tangential	3	0.1	29.0	441	10.6	0.047
		5	Tangential	5	0.1	29.3	457	9.6	0.044
	PUR-1	6	Tangential	1	0.1	29.0	403	12.0	0.048
		7	Tangential	3	0.1	29.3	430	7.9	0.034
		8	Tangential	5	0.1	29.7	476	6.1	0.029
Series 2	Epoxy	9	Tangential	1	0.1	29.3	429	14.0	0.060
		10	Tangential	1	0.5	29.5	586	11.0	0.064
		11	Tangential	1	1.0	30.1	523	11.0	0.058
	PVAc	12	Tangential	1	0.1	29.3	407	14.8	0.060
		13	Tangential	1	0.5	29.5	389	15.3	0.060
		14	Tangential	1	1.0	29.8	351	14.6	0.051
	Urea-2	15	Tangential	1	0.1	29.5	420	15.0	0.063
		16	Tangential	1	0.5	29.5	419	15.3	0.064
		17	Tangential	1	1.0	29.8	417	14.9	0.062
	PUR-2	18	Tangential	1	0.1	29.4	458	14.2	0.065
		19	Tangential	1	0.5	29.8	403	13.5	0.054
		20	Tangential	1	1.0	30.5	452	12.4	0.056

Table 2 Test conditions
Tab. 2 Prüfbedingungen

	Series 1	Series 2
Samples	No. 1–8	No. 9–20
Measurement times after	0, 1, 3, 7, 23, 29, 59, 74 days	0, 1, 3, 7, 14, 21, 34, 49, 70 days
Climatic chamber: climate	20/85	20/90
Scintillator	200 µm Li6	200 µm Li6
Field of view	130 × 130 mm	279 × 279 mm
Pixel size	0.12695 × 0.12695 mm	0.27246 × 0.27246 mm
Exposure time	210 s	21–30 s
Object-detector distance	90 mm	67 mm
Proton flow	~ 1.4 mA	1.07–1.40 mA

case the radial-longitudinal plane) of the sample is exposed to a parallel beam of neutron radiation for a defined time (Table 2). The neutron scintillator converts the neutron signal into visible light, which is led via a mirror onto a cooled 16 bit CCD camera (resolution: 1024 × 1024 pixels, field of view and pixel size as given in Table 2).

After the measurement, the cup with the sample is put into a climatic chamber with a climate of 20 °C and 85% (series 1) and 90% (series 2) relative humidity, respectively. Further measurements take place in an analogous manner after defined time intervals (Table 2). The samples are removed from the climatic chamber only for the few minutes necessary for the radiography measurement.

2.2.2 *Data evaluation*

The attenuation of the neutron radiation within a sample can be described by the exponential law of radiation attenuation

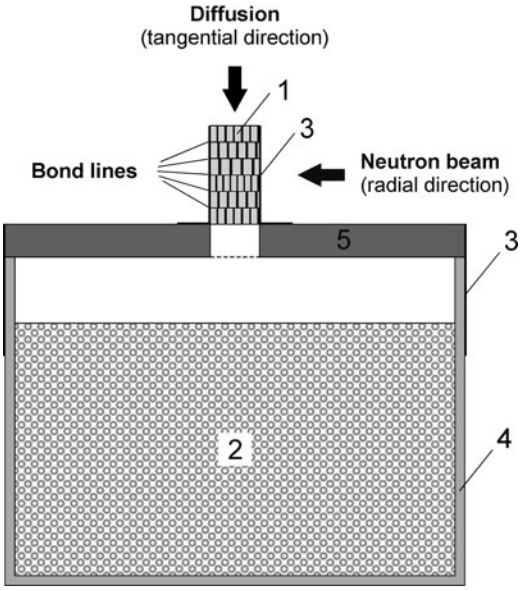

Fig. 1 Test setup of a sample with 5 bond lines. 1 = Sample; 2 = Silica gel; 3 = Aluminium tape; 4 = Glass vessel; 5 = Slotted aluminium plate
Abb. 1 Prüfanordnung einer Probe mit 5 Klebfugen. 1 = Probe; 2 = Silikagel; 3 = Aluminiumband; 4 = Glasgefäß; 5 = geschlitzte Aluminiumplatte

(Beer-Lambert law). For samples with a known thickness this can be used to derive net moisture content in the samples ((1)–(4)).

$$T_w = \frac{I_w}{I_{ow}} = e^{-(\Sigma_w t_w + \Sigma_d t_d)} \tag{1}$$

$$T_d = \frac{I_d}{I_{od}} = e^{-\Sigma_d t_d} \tag{2}$$

$$\frac{T_w}{T_d} = e^{-\Sigma_w t_w} \tag{3}$$

or

$$-\ln\left(\frac{T_w}{T_d}\right) = \Sigma_w t_w \tag{4}$$

Thereby the raw grey-level images, I_w for the wet sample and I_d for the dry sample, were converted to normalised transmission images (T_w for the wet sample and T_d for the dry sample); I_{ow} and I_{od} correspond to the intensity of the respective incident neutron beam, Σ_w and Σ_d represent the attenuation coefficients and t_w and t_d the layer thicknesses of water and wood, respectively.

Since the interaction between neutrons and hydrogenous materials, such as wood, occurs partially as scattering, for quantitative analyses scattering corrections are necessary (Mannes et al. 2009a). Thus, for the evaluation of the experimental data, the raw images were additionally corrected with standard procedures using the scattering correction tool QNI (Hassanein 2006). QNI includes:

- compensation for the offset caused by the background noise of the CCD camera,
- "flat field" correction equalising inhomogeneities of the beam intensity and the scintillator,
- corrections due to sample scattering depending on the material and the distance of the sample to the scintillator and
- corrections due to background scattering where the neutrons are scattered by the experimental facility.

Thereby, the percentage of the background scattering correction (determined with a "black body") was varied by adjusting the images to the dry part of the sample and the area of the aluminium plate (if the sample has already taken up moisture over the whole height, only the area of the aluminium plate was used for adjusting).

The goal of the measurements was to detect the distribution of the water content within the sample in the diffusion direction. First, a profile over the entire height of the dry sample was generated, averaging the values over almost the whole sample width. Then the profiles of the following images (after the defined time intervals of the diffusion experiment) were referenced against the profile gained from the initial (oven-dry) image by dividing the wet profile by the dry profile (3). Due to swelling of the sample during the diffusion process and displacement of the position, the profiles from the following images had to be first adjusted by shifting and linear compressing in order to guarantee that the position of the bond lines coincide with the profile of the initial dry image. The differences between the measurements can be shown via division of the profiles. Application of (4) illustrates the change in water content. To adjust the water content determined via neutron radiation, the mean water content of the last image taken was referenced on the water content obtained by weighing the sample after the measurement was finished. Table 1 shows the mean water content of the samples as MC and as water concentration.

2.2.3 *Determination of the diffusion coefficient*

Evaluation of the diffusion coefficient follows the method described in Mannes et al. (2009b) using a 2nd order linear partial differential equation (PDE) of the diffusion corresponding to Fick's second law. Owing to varying densities in the different wooden layers of a sample due to anatomical properties such as early and latewood, Fick's second law was used in a modified version calculating the diffusion coefficient D depending on MC (cf. Olek and Weres 2007):

$$\frac{\partial M}{\partial t} = \frac{\partial}{\partial x}\left(D\frac{\partial M}{\partial x}\right) \tag{5}$$

where M is the MC in percent, t the time, x the moisture transport direction and D the MC-dependent diffusion coefficient, given in (6):

$$D = D_0 \cdot e^{\alpha \cdot M} \tag{6}$$

where D_0 is the diffusion coefficient at oven-dry state ($M = 0$) and α a constant describing moisture dependency.

Equations (5) and (6) were used for both the wooden part and the bond line applying different parameters for D_0 and α. Thereby, the resolution of the neutron images (Table 2) was the limiting factor, because calculating the diffusion coefficient of the bond lines needs at least one pixel for the calculation. Thus, the pixel size determines the minimum distinguishable thickness of a bond line. Therefore, according to the pixel size, the diffusion coefficients of the bond lines in series 1 were calculated using a thickness of 0.127 mm instead of 0.1 mm. Similarly, in series 2 a thickness of 0.272 mm, 0.545 mm, and 1.09 mm were used instead of 0.1 mm, 0.5 mm, and 1.0 mm, respectively. The high difference between the calculated and measured thicknesses of the thinnest bond line was caused by the fact that the pixel size of series 2 was more than twice as high than of series 1 (Table 2).

The transition between wood and adhesive was presumed to be a C_0 continuous transition. The following boundary conditions were used for the dry (7) and for the moist (8) boundary Γ:

$$M(x,t) = 0 \quad (x,t) \in \Gamma x[0,t] \tag{7}$$

$$\left(-D\frac{\partial M}{\partial x}\right) = \sigma \cdot [M(x,t) - M_\infty], \quad (x,t) \in \Gamma x[b,t] \tag{8}$$

where σ is the surface emission coefficient describing the influence of external resistance on moisture movement (cf. Liu 1989), M_∞ the equilibrium MC and b the height of the sample. Differences between the experimental results M_{exp} and the results for the solved PDE M_{calc} were characterised by an objective function S:

$$S = \sum_{i=1}^{x_n}\sum_{j=1}^{t_n}(M_{\text{exp}}(x,t) - M_{\text{calc}}(x,t))^2 \tag{9}$$

where x_n is the number of local measuring points within the calculation range and t_n the number of test times (Table 2). For the calculation, only the data from the non-deflected wooden areas (bulk wood areas) were taken into account because large deflections occurred around the zones of the bond lines and on the boundaries of the samples (cf. Fig. 2).

The calculation was carried out using a Matlab® (version 7.1, 2005) solver algorithm for partial differential equations and a "Nelder-Mead simplex direct search" optimisation algorithm for the minimisation of the objective function S (Nelder and Mead 1965). This yielded the analysis parameters $D_{o.w}$ and $D_{o.a}$, α_w and α_a (D_0 and α of wood and bond lines, respectively), σ and M_∞.

3 Results and discussion

3.1 Diffusion properties of spruce wood

At low MC, the diffusion coefficient of spruce wood in the radial direction is higher than in the tangential direction. This trend does not change until a MC of about 15% is reached (Fig. 3a). This can be explained by anatomical properties. At low MC, wood rays facilitate the water vapour flow in the radial direction, whereas with higher MC the bound water diffusion within the cell walls, and therefore the late wood zones in the tangential direction become more important (Vanek and Teischinger 1989; Siau 1995). Vanek and Teischinger (1989) investigated diffusion coefficients of spruce wood on the basis of water content profiles within wood samples of steady-state moisture diffusion tests. They measured similar diffusion behaviours in the radial and tangential directions as was obtained within this paper but the change of the trend was already at 8% MC. This difference can be explained by the differing methods and, in regard to the high variation of wood properties, with the fact that within the scope of the presented investigation only one sample per direction could be tested.

The variation of the diffusion coefficients of the bulk wood portions—all in the tangential direction—can be illustrated by evaluating the data of the samples with bond lines (Table 3). Figure 3b shows the mean curves of both series 1 (samples 3–8) and series 2. By comparison with the curve of sample 1 (spruce wood in tangential direction), a lower increase of the diffusion coefficient with increasing MC of both mean curves can be observed. This tendency is intensified for series 2 and may be due to the even higher humidity difference of the climates applied on the two sides of the samples, yielding M_∞ about 20% compared with series 1 (M_∞ about 16%).

3.2 Diffusion properties of bond lines

The influence of the number of bond lines on the diffusion process is shown in Fig. 2. For the samples with a single bond line, the diffusion process has nearly finished after 74 days. Observation of samples with three and five bond lines reveals that the diffusion process just reaches the bottom of the sample, and in the case of sample 8 (1C PUR with 5 bond lines) the water only reaches as far as the fifth bond line. This indicates a high diffusion resistance of the hardened adhesives particularly for the 1C PUR and is also visualised with the steps in the distribution of the MC at each bond line. The high diffusion resistance of the adhesives could be verified with the PDE-calculation (Table 3). Figure 4 shows the calculated diffusion coefficients of the two adhesives depending on MC and compared with the diffusion coefficients of the bulk wood portions. The diffusion coefficient of UF

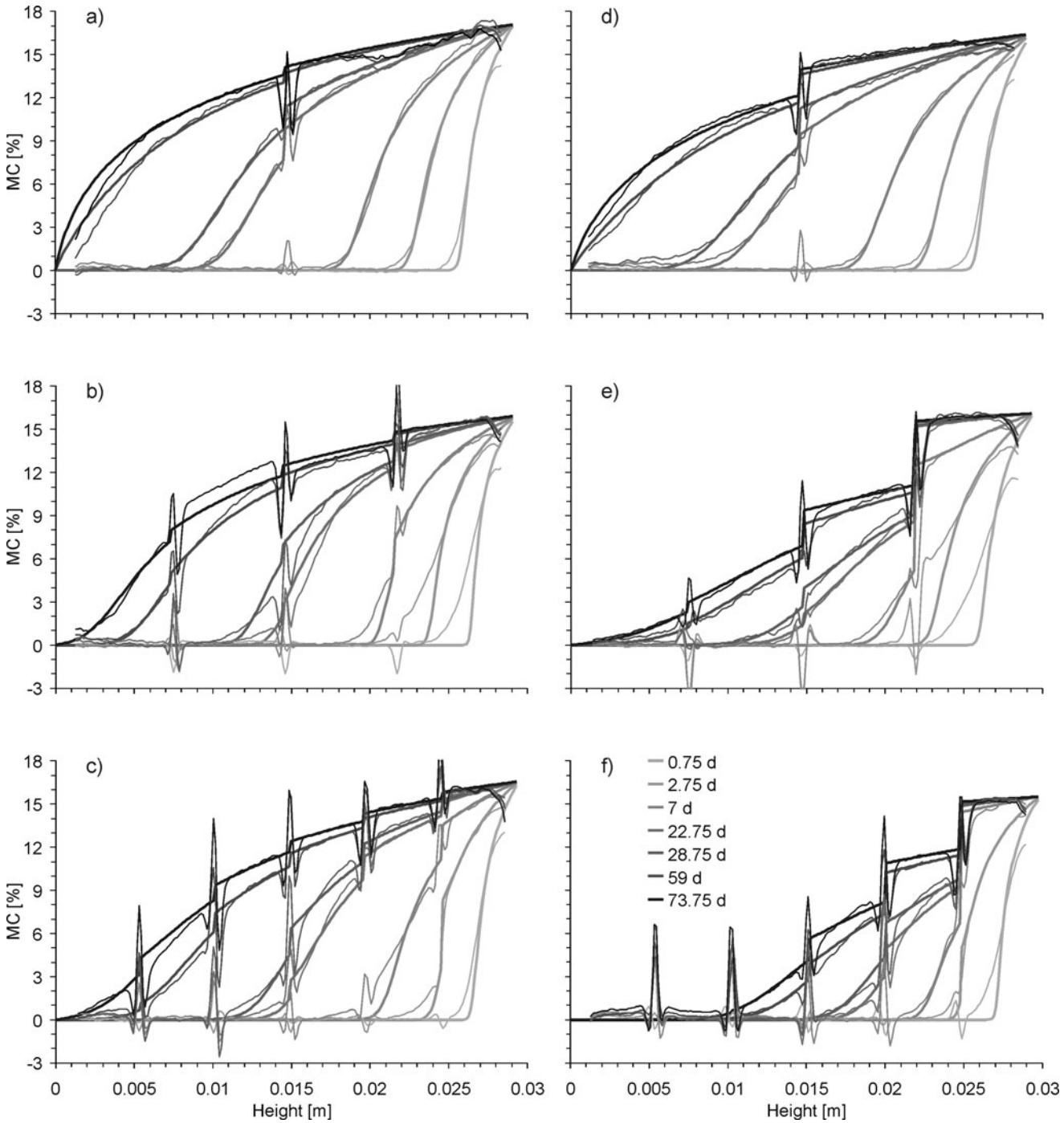

Fig. 2 Vertical profiles of the MC through the samples of series 1 with 1, 3 and 5 bond lines during the diffusion experiment (experimental results = *fine lines*; calculated curves = *fat lines*); (**a–c**) UF, (**d–f**) 1C PUR
Abb. 2 Vertikale Profile des Feuchtegehaltes durch die Proben der Serie 1 mit 1, 3 und 5 Klebfugen während des Diffusionsprozesses (experimentelle Werte = *feine Linien*; berechnete Kurven = *fette Linien*); (**a–c**) UF, (**d–f**) 1K-PUR

over the whole range of the measured MC is about one order of magnitude lower than that of spruce wood. Regarding 1C PUR, the difference between the diffusion coefficients of wood and adhesive increases from one to about three orders of magnitude with increasing MC. Moreover, the diffusion coefficient of 1C PUR shows only a slight dependency on the MC and partly even a negative slope (concerning the increase of the diffusion coefficient with increasing MC). This is contrary to the results of water vapour resistance measurements carried out by Foglia (2006) with the cup method.

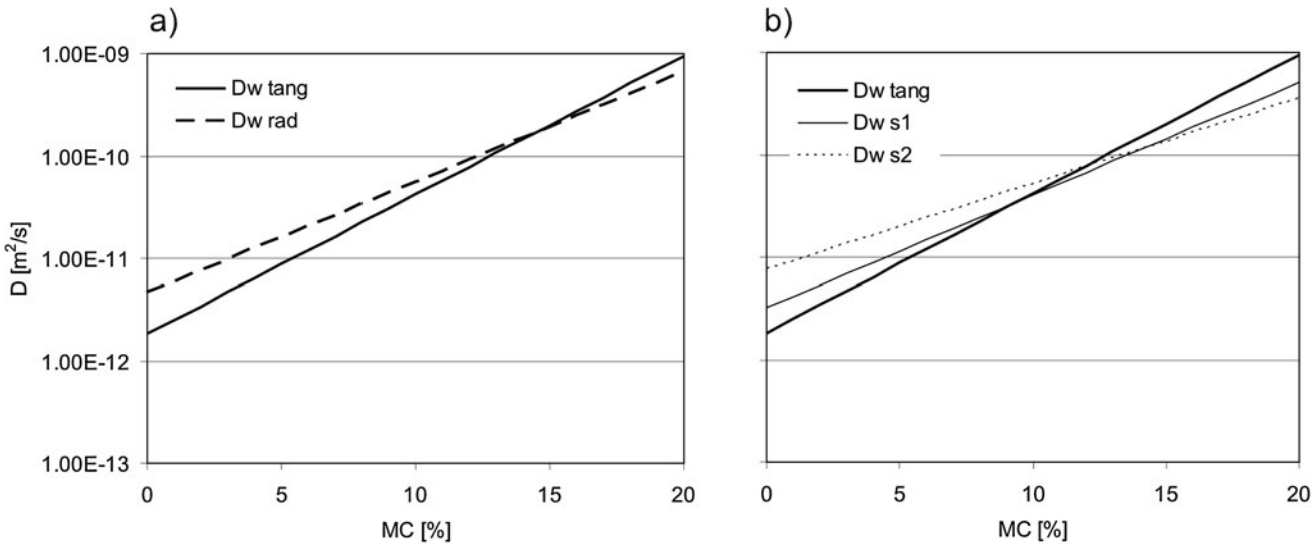

Fig. 3 (**a**) Calculated diffusion coefficients of spruce wood in radial (D_w rad) and tangential (D_w tang) direction; (**b**) Comparison of the diffusion coefficient in tangential direction with the mean diffusion coefficients (D_{ws1}, D_{ws2}) of the bulk wood portions of the samples with bond lines of series 1 (samples 3–8) and series 2

Abb. 3 (**a**) Berechnete Diffusionskoeffizienten von Fichtenholz in radialer (D_w rad) und tangentialer (D_w tang) Richtung; (**b**) Vergleich des Diffusionskoeffizienten in tangentialer Richtung mit den gemittelten Diffusionskoeffizienten (D_{ws1}, D_{ws2}) der reinen Holzbereiche bei den Proben mit Klebfugen von Serie 1 (Proben 3–8) und Serie 2

Table 3 Parameters of the diffusion coefficients of wood and adhesive according to (6)–(9). $D_{o.w}$, $D_{o.a}$ = diffusion coefficients at oven-dry state of wood and adhesive respectively; α_w, α_a = constants describing moisture dependency; σ = surface emission coefficient, M_∞ = equilibrium MC; S = value of the objective function

Tab. 3 Die nach (6)–(9) berechneten Parameter zur Bestimmung der Diffusionskoeffizienten von Holz und Klebstoff. $D_{o.w}$, $D_{o.a}$ = Diffusionskoeffizienten von Holz bzw. Klebstoff bei im darrtrockenen Zustand α_w, α_a = Konstanten, welche die Feuchteabhängigkeit beschreiben; σ = Übergangskoeffizient, M_∞ = Feuchtegehalt im Ausgleichszustand; S = Zielfunktionswert

	Material/adhesive	No.	Bond line (No./Thickness)	$D_{o.w}$ (m²/s)	α_w (–)	$D_{o.a}$ (m²/s)	α_a (–)	σ (m/s)	M_∞ (%)	S
Series 1	Spruce tangential	1	–	1.83E-12	0.313	–	–	5.05E-07	16.0	313
	Spruce radial	2	–	4.67E-12	0.248	–	–	6.19E-07	16.1	1112
	Urea-1	3	1/0.1	3.94E-12	0.232	2.72E-13	0.231	2.10E-06	17.1	344
		4	3/0.1	1.82E-12	0.289	8.70E-13	0.117	6.33E-07	15.9	401
		5	5/0.1	2.85E-12	0.243	3.79E-13	0.181	8.45E-07	16.6	261
	PUR-1	6	1/0.1	4.69E-12	0.228	8.52E-13	0.057	4.73E-07	16.4	307
		7	3/0.1	4.11E-12	0.241	8.71E-13	−0.061	1.28E-06	16.1	234
		8	5/0.1	1.93E-12	0.284	4.47E-13	−0.005	9.17E-07	15.5	220
Series 2	Epoxy	9	1/0.1	1.12E-11	0.149	2.27E-13	0.113	1.32E-07	21.2	330
		10	1/0.5	2.84E-12	0.197	7.57E-13	−0.025	5.73E-08	20.8	394
		11	1/1.0	4.95E-12	0.183	9.55E-13	0.006	5.07E-08	20.4	326
	PVAc	12	1/0.1	1.19E-11	0.147	2.52E-13	0.265	1.24E-07	20.8	402
		13	1/0.5	4.50E-12	0.243	1.51E-12	0.128	4.77E-08	20.3	372
		14	1/1.0	7.31E-12	0.209	1.83E-12	0.135	4.58E-08	20.7	296
	Urea-2	15	1/0.1	8.20E-12	0.187	2.35E-12	0.266	5.09E-08	20.5	354
		16	1/0.5	6.15E-12	0.204	8.96E-12	0.127	6.23E-08	20.6	377
		17	1/1.0	6.43E-12	0.207	2.48E-12	0.309	3.90E-08	20.5	332
	PUR-2	18	1/0.1	6.96E-12	0.188	2.22E-12	0.027	8.69E-08	20.2	286
		19	1/0.5	9.13E-12	0.216	2.98E-12	0.031	4.72E-08	19.7	290
		20	1/1.0	1.11E-11	0.181	3.17E-12	0.056	5.10E-08	19.1	279

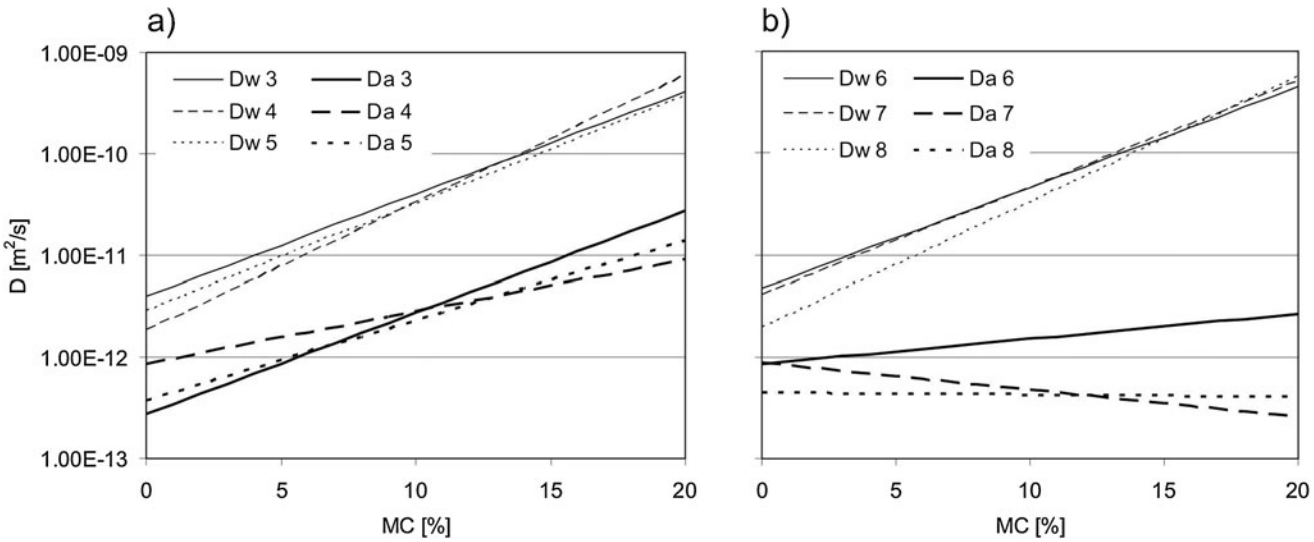

Fig. 4 Calculated diffusion coefficients of the bulk wood portions (D_w) and the bond lines (D_a) of the samples of series 1 depending on MC and the number of bond lines (1, 3 and 5 joints): (**a**) UF (samples 3–5), (**b**) 1C PUR (samples 6–8)
Abb. 4 Berechnete Diffusionskoeffizienten der reinen Holzbereiche (D_w) und der Klebfugen (D_a) bei den Proben von Serie 1 in Abhängigkeit vom Feuchtegehalt und der Klebfugenanzahl (1, 3 und 5 Klebfugen): (**a**) UF (Proben 3–5), (**b**) 1K-PUR (Proben 6–8)

Also for series 2, the diffusion coefficients of the investigated adhesives clearly differ. Furthermore, a small influence of the thickness of the adhesive layer (bond line) was found for all adhesives: the diffusion coefficients increase with increasing thickness (Fig. 5). The diffusion coefficients of PVAc and UF show a high dependency on MC similar to the spruce wood whereas EP and 1C PUR show only low dependency on MC; for EP even the diffusion coefficient partly decreases with increasing MC (Table 3 and Fig. 5). In contrast to EP and 1C PUR, PVAc and UF are highly influenced by water. In contact with water PVAc swells, a fact which reduces the bond resistance; UF degrades as a result of hydrolysis (Dunky and Niemz 2002). Both processes weaken to some extent the integrity of the bond line and thus may cause the increase of the diffusion coefficient with increasing MC. In addition, Hass et al. (2010) investigated the influence of hardening and observed micro cracks within UF joints and pores within PVAc joints due to shrinkage. Dunky and Niemz (2002) also stated that swelling and shrinkage provoke crack formation in UF joints. Measurements of the water vapour diffusion resistance factor of foamed PVAc bond lines show clearly smaller diffusion resistances compared to unfoamed PVAc bond lines due to the high pore ratio (Sonderegger 2010). Therefore, it is conceivable that cracks and pores increase the diffusion coefficient with increasing MC, too.

The comparison of the results of series 2 with series 1 reveals that the diffusion coefficients of both adhesives, 1C PUR and UF, are higher at series 2, so that the diffusion coefficients for UF even are similar to the diffusion coefficients of the bulk wood portions (Figs. 4 and 5). This may be due to the greater difference between the two climates on both sides of the samples and the fact that most of the measured profiles used for the calculation are located on a high MC near the bond line (similar to Fig. 2a) so that the calculation was mainly influenced by a high MC. Moreover, the differences between the 1C PUR adhesives of series 1 and series 2 may also be attributed to the mechanical properties (e.g. different stiffness) of the two adhesives. EP as the adhesive with the highest bond resistance shows the lowest diffusion coefficient and therefore the highest diffusion resistance.

4 Conclusion

Using NI as a non-destructive method with a high sensitivity for hydrogen, it was possible to detect time dependent diffusion processes within wooden samples containing bond lines by localising and quantifying the water content in the diffusion direction.

On the basis of the received data, both the MC dependent diffusion coefficients of the spruce wood as well as of the bond lines were calculated in the form of an exponential function relative to MC with good agreement to the measured data.

The diffusion resistance of the bond lines strongly depends on the adhesive type and on the MC. 1C PUR and EP show up to three orders of magnitude lower diffusion coefficients at high MC compared to spruce wood and have a high barrier effect on water sorption over the whole measured MC range. In contrast, PVAc and UF had a lower barrier effect and clearly depend on the MC (diffusion coefficient increases with increasing MC).

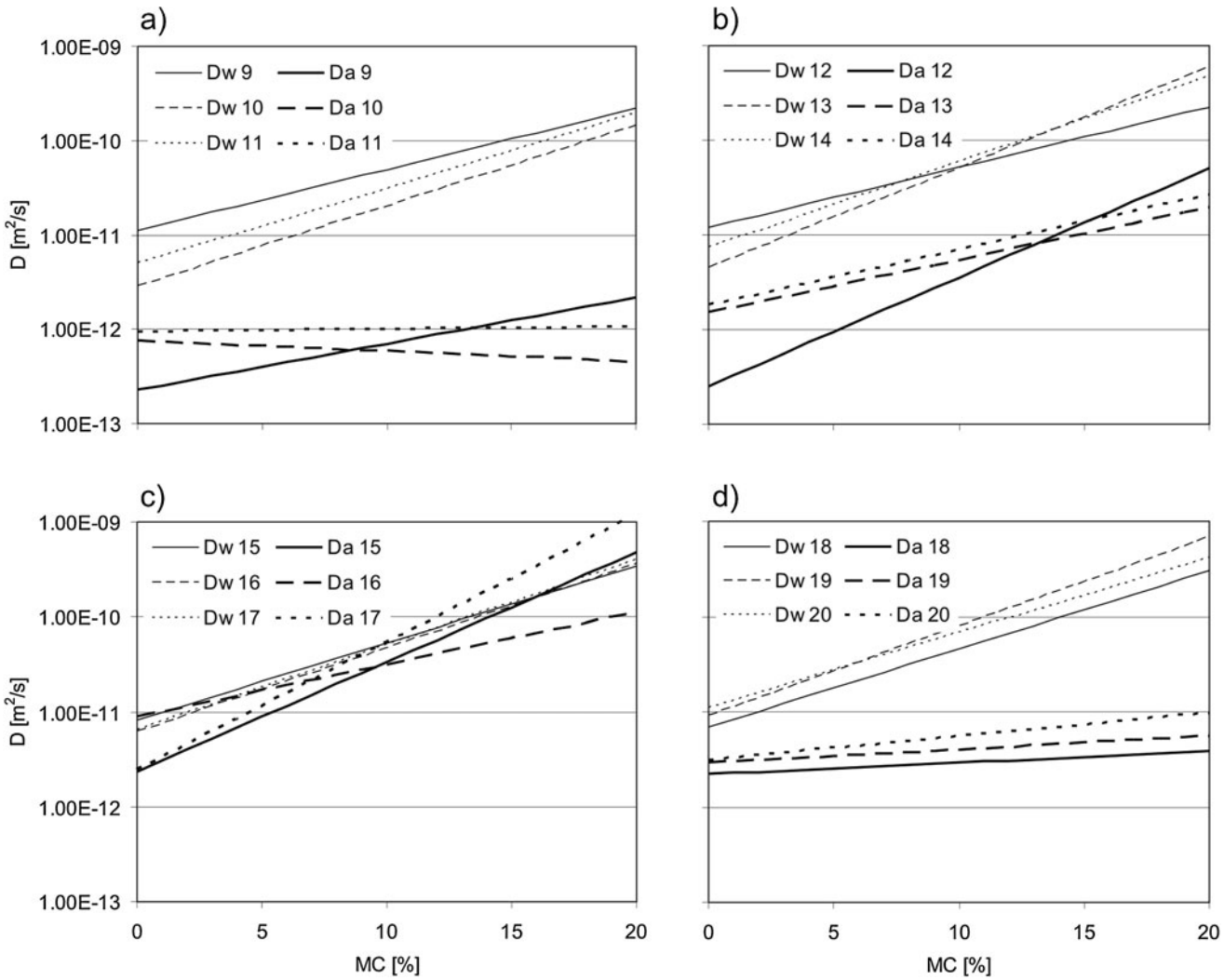

Fig. 5 Calculated diffusion coefficients of the bulk wood portions (D_w) and the bond lines (D_a) of the samples of series 2 depending on MC and the thickness of the bond lines (0.1 mm, 0.5 mm and 1.0 mm, respectively): (**a**) EP (samples 9–11), (**b**) PVAc (samples 12–14), (**c**) UF (samples 15–17), (**d**) 1C PUR (samples 18–20)

Abb. 5 Berechnete Diffusionskoeffizienten der reinen Holzbereiche (D_w) und der Klebfugen (D_a) bei den Proben von Serie 2 in Abhängigkeit vom Feuchtegehalt und der Dicke der Klebfugen (jeweils 0.1 mm, 0.5 mm und 1.0 mm); (**a**) EP (Proben 9–11), (**b**) PVAc (Proben 12–14), (**c**) UF (Proben 15–17), (**d**) 1K-PUR (Proben 18–20)

References

Dunky M, Niemz P (2002) Holzwerkstoffe und Leime: Technologie und Einflussfaktoren. Springer, Berlin/Heidelberg

Foglia A (2006) Untersuchungen zu ausgewählten Einflussfaktoren auf den Diffusionswiderstand von Holzwerkstoffen. Diploma thesis, ETH Zurich, Institute for Building Materials, Wood Physics, Zurich

Frandsen HL, Damkilde L, Svensson S (2007) A revised multi-Fickian moisture transport model to describe non-Fickian effects in wood. Holzforschung 61(5):563–572

Frühwald A (1973) Ein Beitrag zur Kenntnis des diffusionstechnischen Verhaltens von Furnierplatten und kunstharzbeschichtetem Holz. Dissertation, University of Hamburg, Hamburg

Glaser H (1959) Graphisches Verfahren zur Untersuchung von Diffusionsvorgängen. Kältetechnik 11(10):345–349

Hass P, Wittel FK, Mendoza M, Stampanoni M, Herrmann HJ, Niemz P (2010) Adhesive penetration in beech wood. Part I: Experiments. Wood Sci Technol (in press)

Hassanein R (2006) Correction methods for the quantitative evaluation of thermal neutron tomography. Dissertation, ETH Zurich, Zurich

ISO 12572 (2001) Hygrothermal performance of building materials and products—determination of water vapour transmission properties. Geneva

Kollmann F, Côté WA Jr (1968) Principles of wood science and technology, vol I: Solid wood. Springer, Berlin/Heidelberg/New York

Lehmann E, Vontobel P, Scherrer P, Niemz P (2001a) Application of neutron radiography as method in the analysis of wood. Holz Roh-Werkst 59(6):463–471

Lehmann EH, Vontobel P, Wiezel L (2001b) Properties of the radiography facility NEUTRA at SINQ and its potential for Use as European reference facility. Nondestr Test Eval 16:191–202

Liu JY (1989) A new method for separating diffusion coefficient and surface emission coefficient. Wood Fiber Sci 21(2):133–141

Mannes D, Niemz P, Lehmann E (2006) Study on the penetration behaviour of water in corner joints by means of neutron radiography. Wood Res 51(2):1–14

Mannes D, Josic L, Lehmann E, Niemz P (2009a) Neutron attenuation coefficients for non-invasive quantification of wood properties. Holzforschung 63(4):472–478

Mannes D, Sonderegger W, Hering S, Lehmann E, Niemz P (2009b) Non-destructive determination and quantification of diffusion processes in wood by means of neutron imaging. Holzforschung 63(5):589–596

Nelder JA, Mead R (1965) A simplex method for function minimization. Comput J 7(4):308–313

Niemz P, Lehmann E, Vontobel P, Haller P, Hanschke S (2002) Investigations using neutron radiography for evaluations of moisture ingress into corner connections of wood. Holz Roh- Werkst 60(2):118–126

Olek W, Weres J (2007) Effects of the method of identification of the diffusion coefficient on accuracy of modeling bound water transfer in wood. Transp Porous Med 66:135–144

Siau JF (1995) Wood: influence of moisture on physical properties. Virginia Polytechnic Institute and State University, Keene

Skaar C (1988) Wood-water relations. Springer, Berlin/Heidelberg/New York

Sonderegger W (2010) unpublished results

Stamm AJ (1959a) Bound-water diffusion into wood in the fiber direction. For Prod J 9(1):27–32

Stamm AJ (1959b) Bound-water diffusion into wood in across-the-fiber directions. For Prod J 10(10):524–528

Vanek M, Teischinger A (1989) Diffusionskoeffizienten und Diffusionswiderstandszahlen von verschiedenen Holzarten. Holzforsch Holzverwer 41(1):3–6